nature chemical biology

ARTICLE

PUBLISHED ONLINE: 28 NOVEMBER 2010 | DOI: 10.1038/NCHEMBIO.481

Specific Btk inhibition suppresses B cell– and myeloid cell–mediated arthritis

Julie A Di Paolo[1,12,13], Tao Huang[2,12], Mercedesz Balazs[2], James Barbosa[8,13], Kai H Barck[3], Brandon J Bravo[4], Richard A D Carano[3], James Darrow[5,13], Douglas R Davies[6], Laura E DeForge[7], Lauri Diehl[8], Ronald Ferrando[8], Steven L Gallion[9,13], Anthony M Giannetti[4], Peter Gribling[2], Vincent Hurez[2,13], Sarah G Hymowitz[10], Randall Jones[1,13], Jeffrey E Kropf[5,13], Wyne P Lee[2], Patricia M Maciejewski[1,13], Scott A Mitchell[5,13], Hong Rong[1,13], Bart L Staker[6], J Andrew Whitney[1,13], Sherry Yeh[7], Wendy B Young[11], Christine Yu[10], Juan Zhang[2], Karin Reif[2]* & Kevin S Currie[5,13]*

Bruton's tyrosine kinase (Btk) is a therapeutic target for rheumatoid arthritis, but the cellular and molecular mechanisms by which Btk mediates inflammation are poorly understood. Here we describe the discovery of CGI1746, a small-molecule Btk inhibitor chemotype with a new binding mode that stabilizes an inactive nonphosphorylated enzyme conformation. CGI1746 has exquisite selectivity for Btk and inhibits both auto- and transphosphorylation steps necessary for enzyme activation. Using CGI1746, we demonstrate that Btk regulates inflammatory arthritis by two distinct mechanisms. CGI1746 blocks B cell receptor–dependent B cell proliferation and in prophylactic regimens reduces autoantibody levels in collagen-induced arthritis. In macrophages, Btk inhibition abolishes FcγRIII-induced TNFα, IL-1β and IL-6 production. Accordingly, in myeloid- and FcγR-dependent autoantibody-induced arthritis, CGI1746 decreases cytokine levels within joints and ameliorates disease. These results provide new understanding of the function of Btk in both B cell– or myeloid cell–driven disease processes and provide a compelling rationale for targeting Btk in rheumatoid arthritis.

Rheumatoid arthritis is a multifactorial autoinflammatory disease characterized by synovial membrane hyperplasia with infiltration of inflammatory cells, including B cells, T cells and macrophages, as well as cartilage destruction and bone erosion. The success of current therapies (TNFα, IL-6 and IL-1β neutralization, B cell depletion and inhibition of T cell activation) suggests that both adaptive and innate immune system mechanisms are important in disease pathology.

Aspects of B cell–mediated pathology include their role as antigen-presenting cells, their function in lymphoid tissue organization and their production of rheumatoid arthritis–associated autoantibodies. In particular, rheumatoid factor and IgG-containing autoantibodies to cyclic citrullinated proteins (CCP) are detected in the serum of ~75% of rheumatoid arthritis patients[1,2]. Autoantibodies to type II collagen, a major constituent of articular cartilage, are also found in sera (30–70%) and synovial fluid of rheumatoid arthritis patients[3]. Autoantibodies react with autoantigens within the joint, leading to immune complex formation, complement activation and inflammatory cell recruitment. Patients seropositive for rheumatoid factor and anti-CCP often develop more erosive disease and are at risk for increased mortality and morbidity[4].

IgG immune complexes exert their pathogenic effects through activating Fcγ receptors (FcγR), resulting in the initiation of cellular signaling pathways that ultimately trigger inflammatory cytokine production, as well as phagocytic and cytolytic activities[5,6]. The importance of FcγRs in rheumatoid arthritis pathogenesis is supported by the linkage of FcγR polymorphisms with rheumatoid arthritis[6,7] and the striking effects of FcγR deficiency on disease progression in inflammatory arthritis models[8]. Three activating FcγRs in humans (FcγRI, FcγRIIa, FcγRIIIa) and mice (FcγRI, FcγRIII, FcγRIV) have been identified, along with one inhibitory receptor, FcγRIIb. Activating FcγRs are expressed on myeloid lineage and dendritic cells, with macrophages in particular being implicated in mediating the pathogenic functions of immune complexes in arthritis. Indeed, joint macrophage numbers increase during rheumatoid arthritis progression and correlate with severe cartilage destruction[9]. An improved understanding of the molecular mechanisms by which FcγRs trigger macrophage activation may offer new opportunities for therapeutic intervention.

Btk is a member of the Tec family tyrosine kinases and is expressed in all hematopoietic cells except T cells, natural killer cells and plasma cells. Btk contains an N-terminal pleckstrin homology domain, followed by a Src homology 3 domain (SH3), a Src homology 2 domain and a C-terminal kinase domain. Btk is regulated by membrane recruitment via its pleckstrin homology domain, phosphorylation of Tyr551 in the activation loop and

[1]Department of Discovery Biology, CGI Pharmaceuticals, Branford, Connecticut, USA. [2]Department of Immunology, Genentech Inc., South San Francisco, California, USA. [3]Department of Tumor Biology & Angiogenesis, Genentech Inc., South San Francisco, California, USA. [4]Department of Biochemical Pharmacology, Genentech Inc., South San Francisco, California, USA. [5]Department of Medicinal Chemistry, CGI Pharmaceuticals, Branford, Connecticut, USA. [6]Emerald BioStructures, Bainbridge Island, Washington, USA. [7]Department of Assay & Automation Technology, Genentech Inc., South San Francisco, California, USA. [8]Department of Pathology, Genentech Inc., South San Francisco, California, USA. [9]Computational Chemistry CGI Pharmaceuticals, Branford, Connecticut, USA. [10]Department of Protein Engineering, Genentech Inc., South San Francisco, California, USA. [11]Department of Medicinal Chemistry, Genentech Inc., South San Francisco, California, USA. [12]These authors contributed equally to this work. [13]Present addresses: Gilead Sciences, Branford, Connecticut, USA (J.A.D.P., J.B., J.D., S.L.G., J.E.K., P.M.M., S.A.M., H.R., J.A.W., K.S.C.). Cancer Therapy and Research Center at University of Texas Health Science Center San Antonio, San Antonio, Texas, USA (V.H.). *e-mail: kreif@gene.com or kevin.currie@gilead.com

autophosphorylation of Tyr223 in the SH3 domain. Btk is a critical regulator of B cell receptor (BCR) signaling, and mutations in the Btk gene lead to B cell deficiency manifested as X-linked agammaglobulinemia in humans and the related but less severe X-linked immunodeficiency (*xid*) in mice[10–13]. Btk has also been implicated in myeloid lineage cell function, although, with the exception of mast cells and platelets, its biological role is poorly defined[14,15].

Here we describe the characterization and crystal structure of CGI1746 (G-182), which represents a new small-molecule Btk inhibitor chemotype. Unlike previously described Btk inhibitors, CGI1746 exploits binding interactions with an inactive enzyme conformation to deliver over 1,000-fold target selectivity, enabling interrogation of Btk function free from the confounding effects of off-target activity. Using CGI1746, we demonstrate that Btk regulates PLCγ2 phosphorylation and Ca^{2+} release in response to immune complex stimulation of FcγRIII or FcγRIIA in primary murine macrophages or human monocytes, respectively. Importantly, we show that Btk is essential for FcγR-induced inflammatory cytokine production, including TNFα and IL-1β. CGI1746 ameliorated myeloid cell–dependent disease in rodent models of inflammatory arthritis driven by immune complexes and FcγR activation. Furthermore, CGI1746 inhibited B cell activation and prevented arthritis in B cell–dependent collagen-induced arthritis (CIA) models. Our data highlight a dual mechanism of action of Btk inhibition in inflammatory arthritis, comprising suppression of myeloid cell–dependent inflammatory cytokine production and inhibition of B cell–dependent autoantibody production. These mechanistic insights provide a new understanding of the potential role that Btk signaling plays in rheumatoid arthritis and other B cell– and immune complex–mediated disorders.

RESULTS

CGI1746 is a potent and highly selective Btk inhibitor

We synthesized a series of ATP site–directed compound libraries around the imidazo[1,2-a]pyrazine scaffold (**Fig. 1a**). We expected that this ring system would form hydrogen bonds with the hinge via the 8-amino group and N-1 of the bicycle, thus allowing exploration of additional binding interactions via R1 and R2. Screening of these libraries against Btk identified CGI560 (**1**), which showed modest Btk potency (half-maximal inhibitory concentration (IC_{50}) = 400 nM) but promising selectivity (>ten-fold) over an initial panel of 16 kinases[16]. Subsequent hit-to-lead chemistry confirmed the importance of the hydrogen bond donor-acceptor arrangement provided by the amino-imidazopyrazine, identified bioisosteric hinge binding motifs and highlighted the *para* position of the 8-aniline ring as a promiscuous site tolerant of diverse substitutions. Notably, we found the t-butylphenyl amide to be a critical pharmacophore for potency and selectivity. This effort identified CGI1746 (**2**) (**Fig. 1b**)[17] as a potent ATP-competitive Btk inhibitor with a IC_{50} of 1.9 nM, measured at an ATP concentration equal to its experimental K_m value (**Supplementary Fig. 1a**). The importance of the t-butylphenyl amide for Btk binding is indicated by compounds **3**–**7** (**Fig. 1b**). The aniline **3** is essentially inactive, demonstrating that the hinge interaction alone is insufficient for binding. The poor activity of the acetate **4** and the benzylamine **5** demonstrate that the amide carbonyl and the t-butylphenyl group are both required for potent binding, whereas the *meta*-t-butyl isomer **6** and the pyridyl derivative **7** indicate a lipophilic binding pocket of limited size. These observations are consistent with the crystal structure of the CGI1746–Btk complex (see below).

CGI1746 is specific for Btk, with ~1,000-fold selectivity over Tec and Src family kinases (**Supplementary Table 1**). In an ATP-free competition binding assay, the dissociation constant (K_d) for Btk was 1.5 nM, and there was no significant binding to a further 385 nonmutant kinases at 1 μM (**Fig. 1c** and **Supplementary Table 2**). We confirmed this selectivity in enzymatic assays, in which CGI1746 at 1 μM did not significantly inhibit 205 kinases tested, other than Btk (**Supplementary Table 3**). Furthermore, CGI1746 showed negligible off-target activity against 82 nonkinase targets (**Supplementary Table 4**). Thus CGI1746 potently inhibits Btk and shows no significant activity on any of the other 468 discrete targets tested, such that the IC_{50} of CGI1746 for Btk was >980 times lower than the IC_{50} for the second most sensitive kinase, Bmx. The selectivity profile and reversible binding kinetics of CGI1746 are distinct from previously disclosed Btk inhibitors[18].

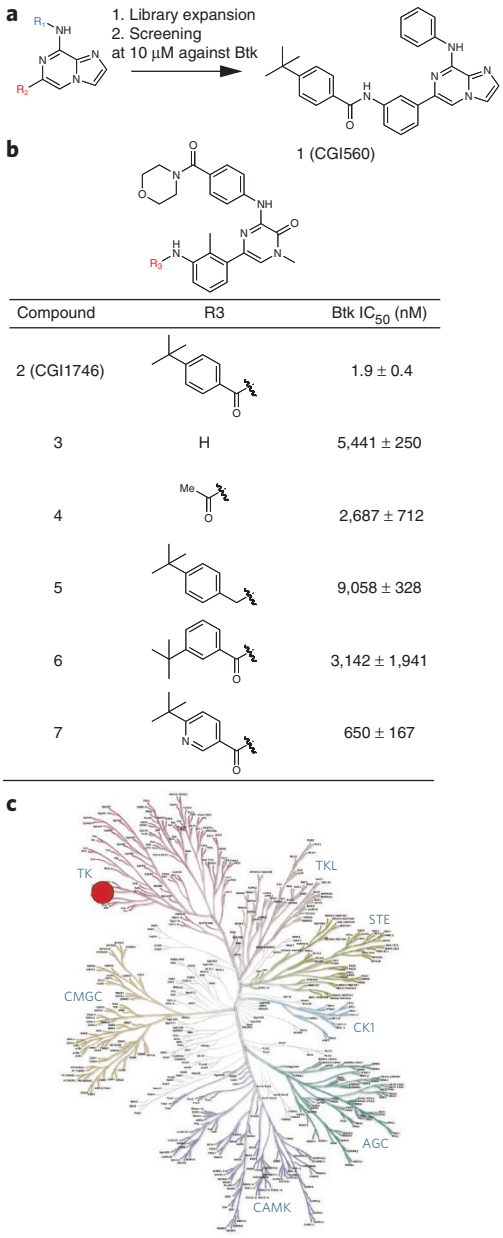

Figure 1 | Discovery and SAR of new Btk inhibitors that bind to the Btk ATP-binding cleft. (**a**) Library design and identification of CGI560 (**1**). (**b**) Structure of CGI1746 (**2**) and SAR for H3 binding. The amide motif and t-butylphenyl group are required for potent Btk inhibition. IC_{50}s were determined at the K_m for Btk and are the mean ± s.e.m. of at least three experiments. (**c**) Kinome binding map of CGI1746 based on an Ambit screen, data provided in **Supplementary Table 2**. CGI1746 only showed significant binding to Btk at 1 μM, indicated by the red circle.

CGI1746 stabilizes an inactive conformation of human Btk

Btk activity is regulated by plasma membrane recruitment and subsequent tyrosine phosphorylation events. Upon receptor activation, phosphorylation of Tyr551 within the activation loop by Src family kinases results in the acquisition of catalytic activity[19] and in a postulated transition from a Src-like inactive[20] to an active conformation. To better understand the unique selectivity of CGI1746, we determined the 1.8-Å crystal structure of CGI1746 bound to the human Btk kinase domain. This structure showed that CGI1746 binds to a Src-like inactive conformation of Btk in which the key activating tyrosine Tyr551 is unphosphorylated and is sequestered from solvent through interactions with CGI1746 and an intramolecular hydrogen bond with Asp521 (**Fig. 2a–c**). CGI1746 binds in an extended conformation, spanning ~15 Å from the hinge interaction to the t-butylphenyl group (**Fig. 2a**). Binding of CGI1746 induces a significant conformational change in Btk, with the position of the Tyr551 hydroxyl group differing by ~18 Å in the CGI1746-bound versus the apo (unbound) human Btk structure (**Fig. 2a**,**c**), resulting in the formation of a large pocket, termed the 'H3' pocket, which is occupied by the t-butylphenyl moiety of CGI1746 (**Fig. 2b**). Multiple structural elements from the Btk catalytic, phosphate-binding and activation loops contribute to this unique binding site. Side chains from Phe413 (P-loop), Leu542, Val546 and Tyr551 (activation loop) contribute to the size and shape of the 'back' and 'top' of the H3 pocket, whereas the 'base' of the pocket is formed by Asn526 and Asp521 from the C-lobe of the kinase. The pocket also includes a structurally important water molecule that is coordinated by hydrogen bonds to the backbone carbonyls of Asp539 and His519 and the backbone amide of Ser543 (**Fig. 2c**).

In addition to the new interactions with the H3 pocket, CGI1746 also productively interacts with the hinge between the N- and C-lobes and exploits polar interactions with the catalytic lysine (Lys430). Specifically, CGI1746 makes two hydrogen bonds to the hinge residue Met477 as well as complementary dipolar interactions between the N-methyl and backbone carbonyl of Glu475 and the hydroxyl group of Thr474 and a bifurcated hydrogen bond with the side chain amino group of Lys430 and a structurally significant water (**Fig. 2c**).

On the basis of the structure-activity relationships (SARs) described above, interactions with the H3 pocket are likely responsible for the selectivity of CGI1746. Although this enzyme conformation has been observed in a recent structure of Btk bound to the pyrrolopyrimidine inhibitor B43, this compound does not occupy the H3 pocket and is a nonselective inhibitor[21]. Divergence of kinase sequences in this area and the possible inability of other kinases to adopt this conformation in which an inhibitor molecule can simultaneously form favorable interactions with both the 'hinge' and the H3 pocket probably represent the structural origins of CGI1746 specificity.

To assess whether the H3 pocket is formed with the less selective Abl-Src-Btk inhibitor dasatinib, we determined the structure of Btk bound to dasatinib to 1.95-Å resolution (**Fig. 2d**,**e** and **Supplementary Table 5**). In contrast to the Btk–CGI1746 structure, when Btk binds dasatinib, the activation loop is not ordered (as shown by an absence of electron density for residues 545–558), the H3 pocket is not formed, and thus Tyr551 is not sequestered. This result is consistent with a recently reported structure of dasatinib bound to the Y551E Btk mutant[21]. Consistent with these observations, dasatinib is a highly promiscuous kinase inhibitor[22]. Surface plasmon resonance data showed that CGI1746 binds to the unactivated form of Btk with 32-fold greater affinity than the activated form (K_D = 2.9 nM and 94.1 nM, respectively) and that this affinity loss with activated Btk is exclusively due to an increased off-rate (**Supplementary Fig. 1b**

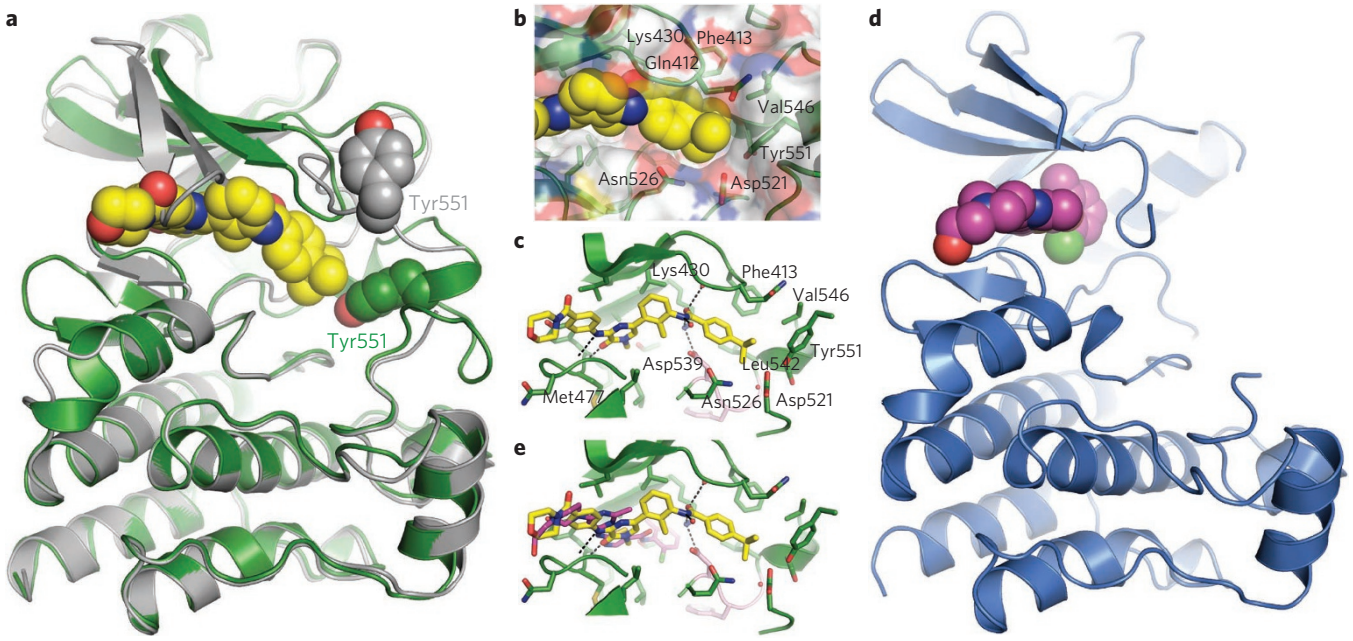

Figure 2 | Structural basis of CGI1746 selectivity. (**a**) Btk undergoes a conformational change upon binding CGI1746 resulting in sequestration of Tyr551. Ribbon diagram of the crystal structure of human Btk bound to CGI1746 (green and yellow) superimposed on human apo Btk (gray). The Tyr551 residues from each structure are shown as spheres. (**b**) Closeup view of the occupation of the H3 pocket by the t-butylphenyl moiety of CGI1746. Btk is shown as a transparent surface with residues of interest including Tyr551 rendered as sticks. (**c**) CGI1746 binds to Btk in an extended conformation and interacts with both the Btk 'hinge' and the H3 pocket. Side chains within 4.2 Å of CGI1746 are shown as sticks. The DGF motif is shown as sticks and colored pink. Select hydrogen bonds are shown as dashed lines. All residues mentioned in the text are labeled with the exception of Thr474, Glu475, His519 and Ser543, which are obscured by CGI1746 in this orientation. (**d**) Dasatinib (magenta) binds to Btk (blue) in a typical type I inhibitor orientation. Btk is shown in the same orientation as in **a**. The activation loop including Tyr551 is not ordered in this structure, and the H3 pocket is not formed. (**e**) Comparison of the dasatinib (magenta) and CGI1746 (yellow) binding modes. Btk and CGI1746 are shown as in **c**.

and **Supplementary Table 6**). The conformational selectivity of CGI1746 is likely because of favorable interactions with the H3 pocket in the inactive state that are not possible in the active state in which Tyr551 phosphorylation prevents close association of the activation loop with H3. In contrast, dasatinib binds with equal affinity to unactivated and activated forms of Btk (K_D = 0.3 and 0.4 nM, respectively).

This combination of chemical, biophysical and structural data will facilitate rational design of next generation selective Btk inhibitors with enhanced physicochemical and absorption, distribution, metabolism and elimination properties.

CGI1746 inhibits B cell signaling and functional effects

To determine the functional consequences of selective Btk inhibition, we evaluated the ability of CGI1746 to inhibit BCR-induced Btk activation and downstream signaling in human and murine B cells. Upon BCR ligation, transphosphorylation of Btk Tyr551 is followed by autophosphorylation at Tyr223 in the SH3 domain, then activated Btk transphosphorylates PLCγ2 on Tyr1217, one of the major regulatory residues involved in calcium mobilization[23]. CGI1746 potently inhibited all three anti-IgM–induced phosphorylation events in both human and murine B cells with an average IC_{50} of 2.9 nM in human B cells (**Fig. 3a** and **Supplementary Figs. 2** and **3**). These results demonstrate that the sequestration of Tyr551 observed in the crystal structure prevents access by upstream kinases (likely Lyn) and subsequent catalytic activation of Btk. CGI1746 also reduced the basal phosphorylation levels of Btk Tyr551 and Tyr223 but not the basal phosphorylation of PLCγ2 Tyr1217, indicating that tonic PLCγ2 Tyr1217 stimulation through the BCR is not dependent on Btk. In agreement with its effect on BCR-induced PLCγ2 phosphorylation, CGI1746 treatment abrogated Ca^{2+} signaling after BCR engagement in a dose-dependent manner (**Fig. 3b**). Furthermore, CGI1746 partially inhibited activation-induced MAP kinase phosphorylation of Erk2 Thr185 and Tyr187, Jnk Thr183 and Tyr185 and p38 Thr180 and Tyr182 in primary human and murine B cells (**Fig. 3a** and **Supplementary Figs. 2** and **3**). Finally, Btk inhibition also blocked BCR-induced nuclear translocation of the classical NFkB pathway transactivators p65 RelA and c-rel in human or murine B cells (**Fig. 3c**,**d** and **Supplementary Fig. 4**).

Functionally, CGI1746 completely inhibited anti-IgM–induced murine and human B cell proliferation, with IC_{50}s of 134 nM and 42 nM, respectively, but had no effect on anti-CD3– and anti-CD28–induced T cell proliferation (**Fig. 3e**). As memory B cell activation may contribute to autoimmunity, we also assessed the ability of CGI1746 to inhibit anti-IgG–triggered B cell proliferation in isotype-switched $CD27^+IgG^+$ human B cells. CGI1746 potently inhibited the proliferation of $CD27^+IgG^+$ B cells isolated from the tonsils of four human donors with an average IC_{50} of 112 nM (**Fig. 3f**).

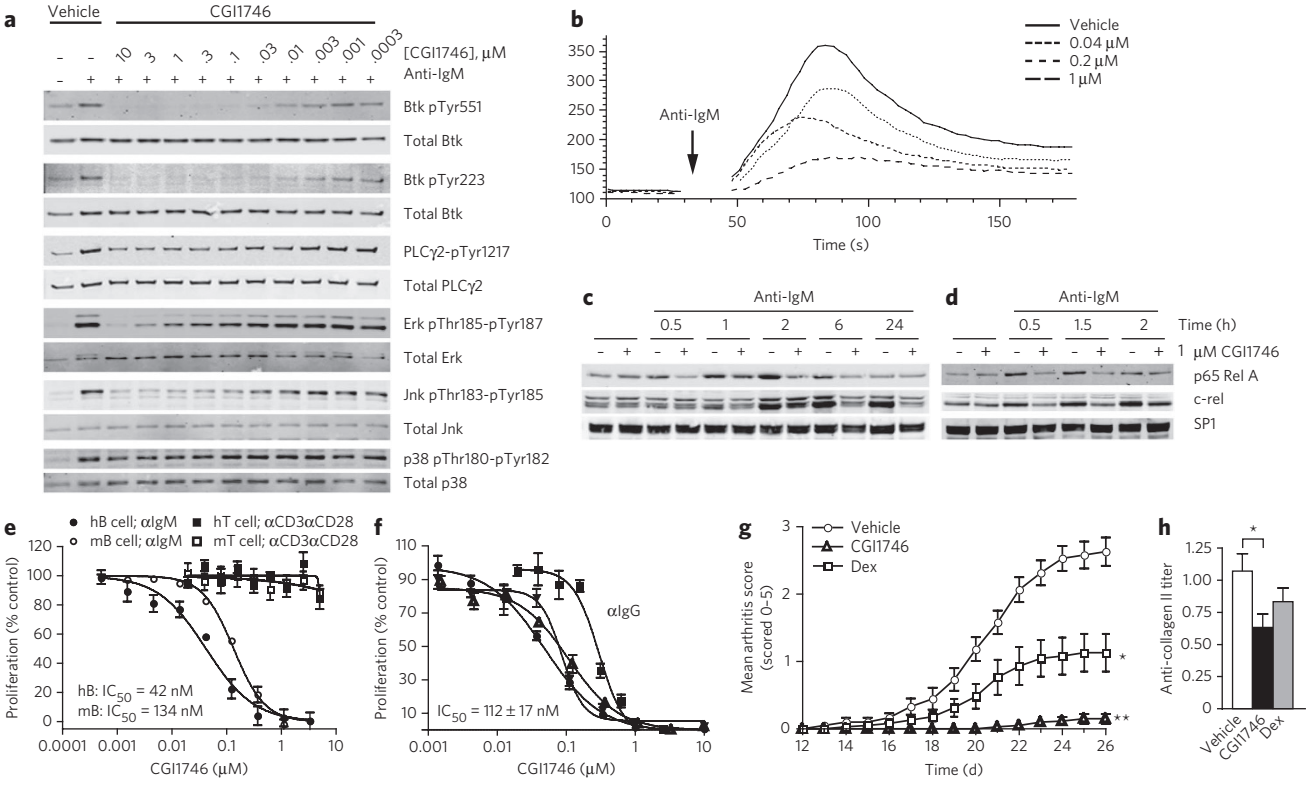

Figure 3 | CGI1746 blocks BCR-mediated responses in primary human and murine B cells and is efficacious in prophylactic CIA. (**a**) Concentration-dependent inhibition by CGI1746 in primary human B cells of anti-IgM $F(ab')_2$-mediated phosphorylation of Btk Tyr223, Btk Tyr551, PLCγ2 Tyr1217 (at 2 min), Erk Thr185 and Tyr187 (5 min), JNK Thr183 and Tyr185, and p38 Thr180 and Tyr182 (10 min). Quantification and full blots in **Supplementary Figure 2**. (**b**) Ca^{2+} flux following stimulation of human B cells with anti-IgM $F(ab')_2$ in the presence of indicated CGI1746 concentrations. Arrow indicates stimulus added. (**c**,**d**) Nuclear translocation of p65 Rel A and c-rel in response to BCR activation in human (**c**) or mouse (**d**) B cells at the indicated times. Full blots in **Supplementary Figure 4**. (**a**–**d**) A representative experiment of at least three experiments is shown. (**e**) Percentage proliferation of human or mouse B cells to anti-IgM $F(ab')_2$ and of human or mouse T cells to plate-bound anti-CD3 plus anti-CD28. Data are mean ± s.e.m. of three experiments. (**f**) Effect of various concentrations of CGI1746 on the proliferation of $CD27^+IgG^+$ human tonsil B cells isolated from four individual donors and stimulated with anti-IgG $F(ab')_2$ for 72 h in duplicate or triplicate (mean ± s.e.m.). (**g**) Prophylactic treatment with CGI1746 protects from collagen-induced arthritis in B10RIII mice. Mean clinical scores (0–5 per paw, averaged per animal, n = 15 per group) were followed from day 12 (treatment start) to day 26. Average daily clinical score in CGI1746 or dexamethasone-treated mice compared with vehicle control: $^*P$ = 0.0002; $^{**}P$ < 0.0001. (**h**) Total IgG anti-collagen II antibody titers at day 26. $^*P$ < 0.02.

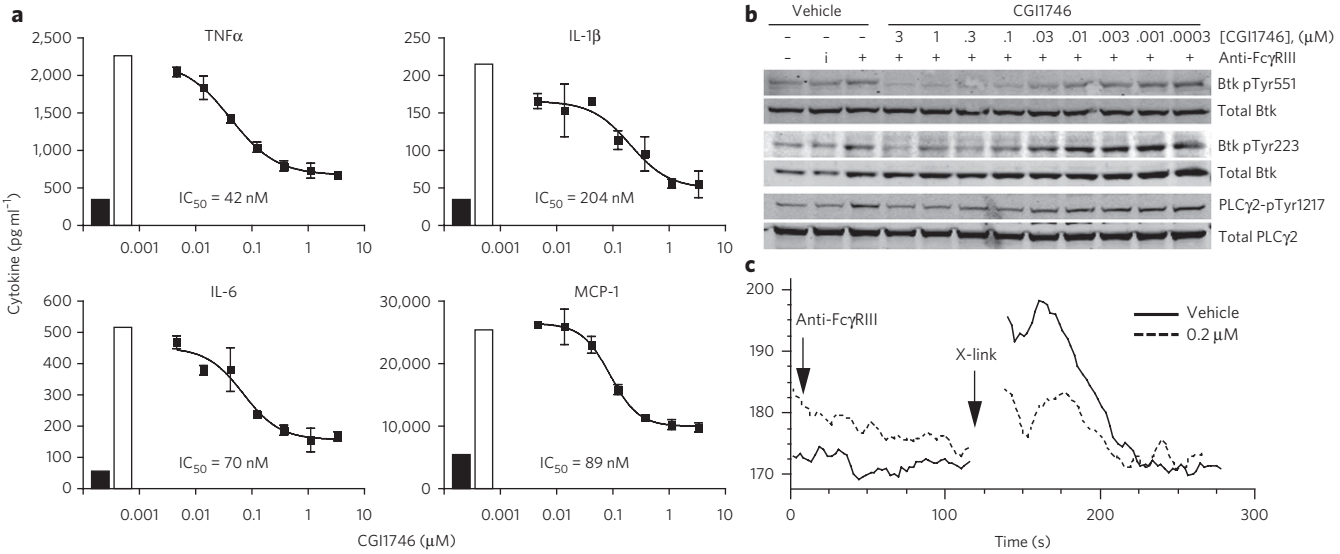

Figure 4 | CGI1746 blocks FcγR-induced signaling and inflammatory cytokine production in murine macrophages. (**a**) Cytokine production as indicated in BMM activated by plate-bound anti-FcγRIII monoclonal antibodies in the absence or presence of indicated concentrations of CGI1746. Data are shown as mean ± s.e.m. of duplicate measurements. Black columns show unactivated and white columns activated conditions in the presence of vehicle control. (**b**) Concentration-dependent inhibition by CGI1746 of anti-FcγRIII–induced phosphorylation of Btk Tyr223, Btk Tyr551 and PLCγ2 Tyr1217 (at 2 min). BMM were incubated with anti-FcγRIII or isotype control monoclonal antibodies at 4 °C and subsequently cross-linked at 37 °C with goat anti-mouse $F(ab')_2$. Quantification and full blots in **Supplementary Figure 7**. (**c**) Calcium mobilization by FcγRIII in BMM. BMM were stimulated with anti-FcγRIII monoclonal antibodies and then cross-linked with goat anti-mouse $F(ab')_2$ in the presence of 0.2 μM CGI1746 or vehicle control. Arrows indicate stimulus added. (**a**–**c**) A representative experiment of at least two experiments is shown.

Btk inhibition abrogates B cell–dependent arthritis

B cell depletion in a prophylactic treatment regimen, or B cell deficiency, prevents autoantibody production and the development of CIA in mice[24]. To test the effect of Btk inhibition on disease onset in CIA, we treated B10.RIII mice prophylactically (day 12 dosing start) with CGI1746 (100 mg kg^{-1}, subcutaneous (SC), twice-daily dosing (BID)) or dexamethasone (0.2 mg kg^{-1}, SC, once-daily dosing (QD)) as a positive control. The 100 mg kg^{-1} SC BID dose covered the IC_{90} for Btk inhibition for about 50% of the dosing period, based on the *in vitro* concentrations of CGI1746 required to inhibit Btk Tyr223 phosphorylation in murine whole blood and the plasma concentrations achieved *in vivo* (**Supplementary Fig. 5**). Treatment with CGI1746 resulted in significant inhibition (97%) of overall clinical arthritis scores (**Fig. 3g**) that was superior to dexamethasone treatment (56% inhibition). Consistent with an effect on B cells, CGI1746 treatment significantly reduced anti–collagen II (CII) titers (**Fig. 3h**). Thus, in agreement with results in *xid* mice[25], Btk contributes to the elicitation phase of CIA when B cells play a critical role, although effects on additional cell types including myeloid cells cannot be excluded.

CGI1746 inhibits FcγR but not TLR function in macrophages

We next examined the influence of Btk inhibition on Fc receptor function and inflammatory cytokine production, which are involved in rheumatoid arthritis pathogenesis. Given the central role of macrophages in rheumatoid arthritis pathology, we determined whether Btk is necessary for immune complex–mediated inflammatory cytokine production in macrophages. Although Btk has been implicated in regulating FcγR-mediated phagocytosis (ref. 26; for review, see ref. 14), the role of Btk in FcγR signaling and cytokine production has not been studied in detail. We confirmed that murine bone marrow–derived macrophages expressed high levels of FcγRI, FcγRIIb and FcγRIII, as well as substantial levels of FcγRIV mRNA (**Supplementary Fig. 6a**). Stimulation of macrophages with immobilized immune complexes resulted in robust TNFα production that CGI1746 inhibited in a dose-dependent manner with an IC_{50} of 25 nM (**Supplementary Fig. 6b**). FcγRI-deficient macrophages, but not FcγRIII-deficient macrophages, produced TNFα in response to stimulation with mIgG1-containing immune complexes (**Supplementary Fig. 6b**). To test whether inhibition of Btk abrogates cytokine production in response to FcγRIII activation, we stimulated macrophages with immobilized anti-FcγRIII monoclonal antibodies Specific activation of wild-type or FcγRI- but not FcγRIII-deficient macrophages with anti-FcγRIII monoclonal antibodies triggered TNFα, IL-1β, IL-6 and MCP1 production that CGI1746 potently inhibited (**Fig. 4a** and **Supplementary Fig. 6c**). CGI1746 also prevented the phosphorylation of activating tyrosine residues on both Btk and PLCγ2 after FcγRIII stimulation but had no significant effect on Erk and Jnk phosphorylation (**Fig. 4b** and **Supplementary Figs. 6d,e** and **7**). Furthermore, CGI1746 suppressed Ca^{2+} mobilization (**Fig. 4c**). Thus Btk is activated downstream of FcγRIII and is essential for inflammatory cytokine production in response to immune complex stimulation. In contrast to FcγRIII-induced cytokine production, Btk inhibition by CGI1746 did not significantly reduce TLR2- or TLR4-mediated TNFα and IL-6 production in macrophages (**Supplementary Fig. 8**).

Btk regulates cytokine levels in myeloid cell arthritis

To determine the effect of selective Btk inhibition on myeloid cell–dependent pathogenesis of autoantibody-mediated arthritis, we evaluated CGI1746 in SCID mice in the passive anti-collagen II antibody–induced arthritis (CAIA) model that requires FcγRs[27]. Although marked arthritis developed in SCID mice treated with vehicle (**Fig. 5a**), CGI1746-treated mice did not develop measurable disease, confirming that Btk contributes to immune complex–triggered disease pathogenesis that is independent of B and T cells. Analysis of local inflammatory cytokine production in the joints showed that CGI1746 treatment substantially reduced TNFα,

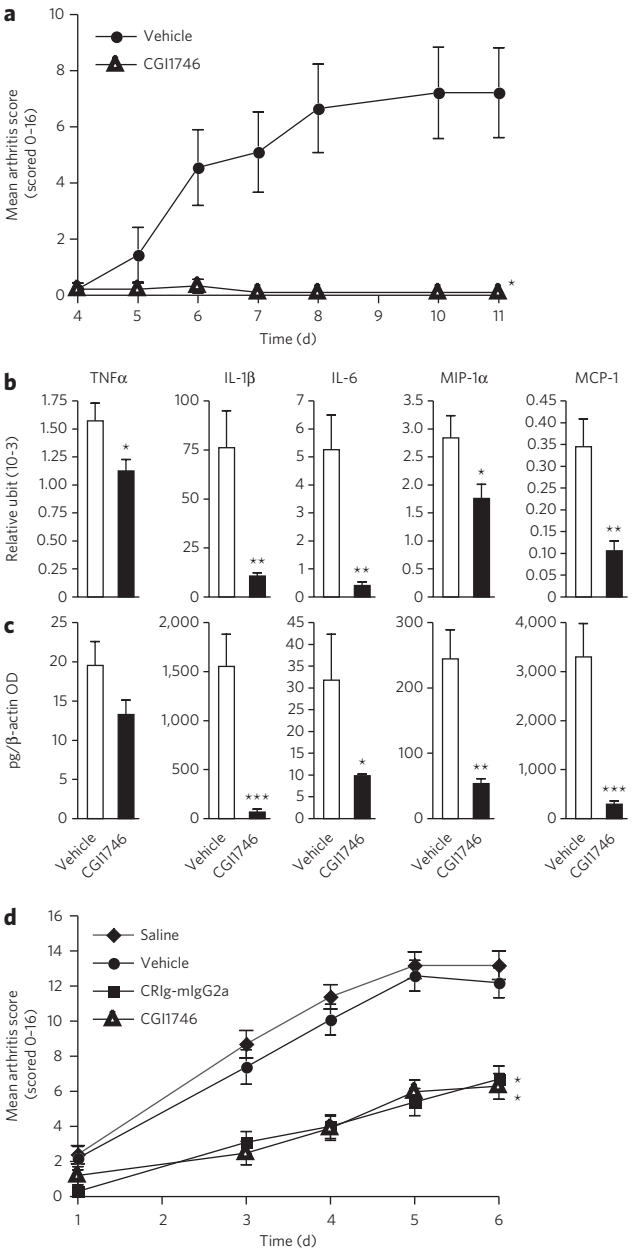

Figure 5 | Administration of CGI1746 inhibits the development of myeloid cell–dependent arthritis after transfer of arthritogenic antibodies and blocks inflammatory cytokine production. (**a**) Arthritis was induced in SCID mice with a cocktail of arthritogenic anti-collagen antibodies on day 0. Mice (n = 10 per group) were treated subcutaneously twice daily with 100 mg kg^{-1} CGI1746 or vehicle control starting the day before antibody injection. Data are presented as the mean clinical score ± s.e.m. *Average daily clinical score P = 0.0015 for CGI1746 compared to vehicle control group. (**b**,**c**) Joint expression of the indicated cytokine mRNA (**b**) or protein (**c**), extracted from paws collected on day 11 from mice of the study in **a** (n = 9 per group for mRNA or protein). mRNA cytokine expression was normalized to RPL19 internal control and protein concentrations were normalized to β-actin levels. (**b**,**c**) *P < 0.05, **P < 0.005, ***P < 0.0005 compared to vehicle-treated control group. (**d**) Mean clinical scores ± s.e.m. of Balb/c mice (n = 10 per group) injected with arthrogenic K/BxN serum on day 0 and treated with 100 mg kg^{-1} CGI1746 (SC, BID), vehicle control, an alternative pathway complement inhibitor CRIg-Fc (100 μg mouse^{-1}, SC, daily) or saline control starting the day before serum transfer. *Average daily clinical score P = 0.0001 for CGI1746 compared to vehicle control group and for CRIg-mIgG2a compared to saline control.

IL-1β and IL-6, as well as MCP1 and MIP-1α on both the mRNA and protein level at the end of the study (**Fig. 5b**,**c**). The effect on TNFα levels was less pronounced, which is in agreement with published data that TNFα plays a role early but not late in this disease model[28,29]. There was no effect on circulating anti-collagen antibody levels (**Supplementary Fig. 9**), indicating that CGI1746 did not interfere with macrophage-mediated clearance of antibodies or antibody complexes. CGI1746 was also efficacious in the K/BxN arthritogenic serum transfer model, a second autoantibody-mediated model of the effector phase of autoimmune arthritis that is driven by immune complexes and complement (**Fig. 5d**). These data show that Btk is essential for myeloid cell cytokine production within joints during immune complex–mediated arthritis and identify Btk as a central player in the effector phase of inflammatory arthritis.

Btk inhibition ameliorates established arthritis

We next evaluated whether Btk inhibition is efficacious during the effector phase of a more complex CIA model, when B cells cease to play a role and TNFα is essential for disease progression. In preventive studies, when treatment started 3 d after secondary collagen immunization (day 24), CGI1746 significantly inhibited disease (P < 0.0001) and showed comparable efficacy to TNFα blockade (**Fig. 6a**). At study termination, metarso- and metacarpophalangeal paw joints showed a significant decrease in bone loss, proliferative synovitis, subsynovial pannus formation and cartilage destruction in mice treated with CGI1746 or a combination of TNFRII-Fc and methotrexate compared to control groups (**Fig. 6b**,**c**). Finally, CGI1746 significantly reduced clinical scores and inhibited joint inflammation in mice or rats with established disease (**Fig. 6d**,**e** and **Supplementary Fig. 10**), further demonstrating an important role for Btk in the effector phase of inflammatory arthritis.

Btk is essential for FcγR function in human monocytes

To evaluate whether murine pathways are conserved in human, we evaluated Btk's role in inflammatory cytokine production in human monocytes. CGI1746 potently inhibited TNFα, IL-1β and, to a lesser extent, IL-6 (three- to eight-fold higher IC_{50}) production in human monocytes stimulated with immobilized (**Fig. 7a**) or soluble (**Supplementary Fig. 11a**) immune complexes. Anti-FcγRIIa–blocking monoclonal antibodies prevented activation by immobilized immune complexes (**Fig. 7b** and **Supplementary Fig. 11b**,**c**) whereas anti-FcγRIIIa– or anti-FcγRI–blocking monoclonal antibodies had no effect in most donors (partial effects observed in subset of donors, see **Supplementary Fig. 11c**). This demonstrates that Btk mediates FcγRIIa-induced inflammatory cytokine production in human monocytes. We next examined the effects of Btk inhibition on signaling pathways downstream of FcγRIIa in human monocytes activated by immune complexes. Similar to the results obtained following BCR stimulation in B cells, CGI1746 prevented activation-induced phosphorylation of Btk Tyr551, Btk Tyr223 and PLCγ2 Tyr1217 and partially inhibited Erk Thr202 and Tyr204, Jnk Thr183 and Tyr185, and p38 Thr180 and Tyr182 phosphorylation (**Fig. 7c** and **Supplementary Figs. 11d** and **12**). Furthermore, CGI1746 blocked Ca^{2+} flux downstream of FcγRIIa in a dose-dependent manner (**Fig. 7d**). These results demonstrate that Btk plays an important role in activating FcγR-mediated inflammatory cytokine production in human monocytes.

DISCUSSION

Btk has attracted considerable interest as a drug target in autoimmune disease. Here, we describe the discovery and characterization of a new, highly selective small-molecule inhibitor of Btk, CGI1746 (G-182). The exceptional selectivity of CGI1746 compared to previously reported Btk inhibitors[18] provides the first opportunity to dissect the role of Btk in cell signaling pathways and its relevance

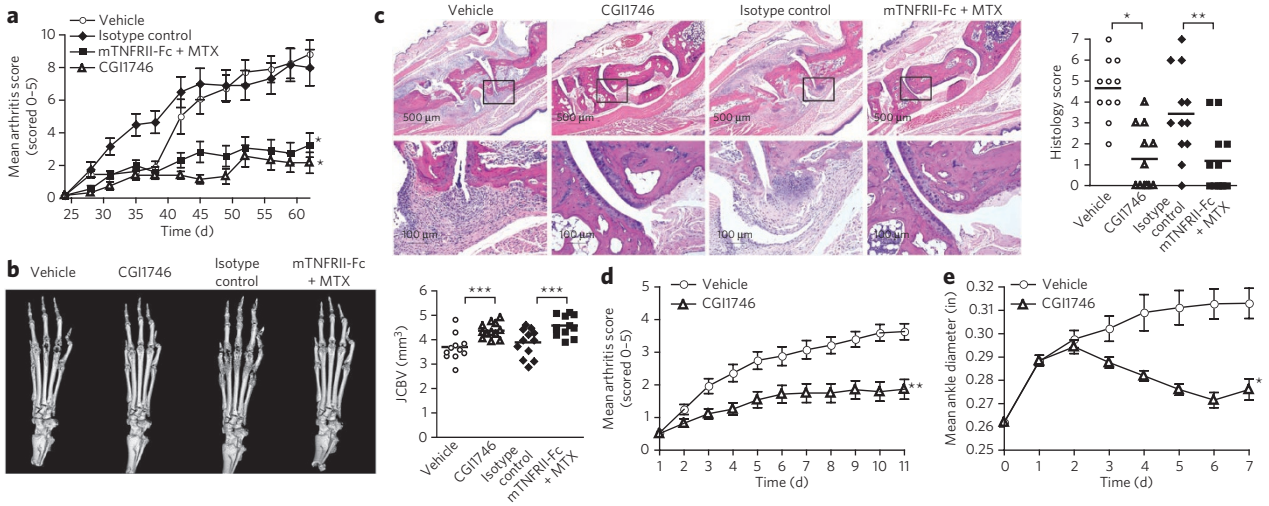

Figure 6 | Therapeutic efficacy of CGI1746 in collagen-induced arthritis. (**a**) Mean clinical scores of DBA/1J mice treated with 100 mg kg^{-1} CGI1746 (SC, BID) or 4 mg kg^{-1} TNFRII-Fc plus 3 mg kg^{-1} methotrexate (MTX) (three times per week) starting day 24 (mean ± s.e.m., n = 12 per group). *Average daily clinical score $P < 0.0001$ for either CGI1746 or TNFRII-Fc compared to their respective control group. (**b**) Joint cortical bone volume (JCBV), as determined by microcomputed tomography analysis of metatarsophalangeal and metacarpophalangeal joints. Mircocomputed tomography renderings show representative mouse hind paws from each treatment group. Bar represents average; symbols represent individual animals. (**c**) Histological comparison of representative hematoxylin and eosin stains from each treatment group of hind paws spanning metatarsal, tarsal and calcaneous bones. Lower panels represent outlined boxes from upper panel at 5× original magnification. Scale bars: 500 µm (upper panel) and 100 µm (lower panel). Graph shows histological scores from the experiment in **a**. Bar represents average; symbols represent individual animals. (**b**,**c**) *$P < 0.005$, **$P < 0.0005$, ***$P < 0.0001$ compared to respective control-treated group. (**d**,**e**) Efficacy of CGI1746 in therapeutic treatment conditions. (**d**) Treatment of B10RIII mice with CGI1746 (100 mg kg^{-1}, SC, BID) or vehicle control was started after arthritis developed (rolling enrollment) and continued for 10 days. (**e**) Treatment of Lewis rats with CGI1746 (100 mg kg^{-1}, SC, BID) began when arthritis was established and continued until end of study. (**d**,**e**) Data points are shown as mean ± s.e.m. (n = 15 per group); terminal clinical score, **P = 0.0001; *$P < 0.001$.

to different states of inflammatory disease in a temporal fashion. Using CGI1746 we show a central role for Btk in BCR and FcγR function and demonstrate that selective, reversible pharmacological inhibition of Btk enzyme activity suppresses B cell– and myeloid cell–mediated inflammatory arthritis.

CGI1746 is the first Btk inhibitor that binds to and stabilizes an inactive conformation of Btk through induction and occupation of an H3 binding pocket. Consequently, Tyr551 is internalized and CGI1746 potently inhibits the transphosphorylation of this activating residue through a Btk-specific mechanism. Although the inactive

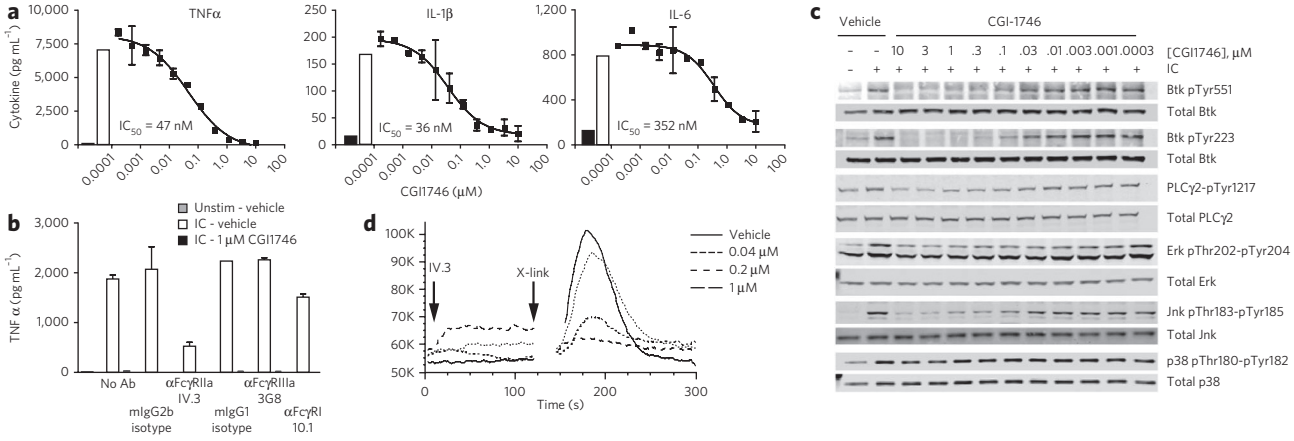

Figure 7 | CGI1746 blocks FcγR-induced signaling and inflammatory cytokine production in human monocytes. (**a**) Cytokine production in human monocytes activated with immobilized anti-HSA immune complexes in the absence or presence of indicated concentrations of CGI1746. (**b**) TNFα production of human monocytes pretreated with 30 µg ml^{-1} anti-FcγRIIa–blocking monoclonal antibodies (clone IV.3), anti-FcγRIIIa–blocking monoclonal antibodies (clone 3G8), anti-FcγRI–blocking monoclonal antibodies (clone 10.1) or respective isotype control antibodies and plated on anti-HSA immune complex–covered surfaces. (**a**,**b**) Data are shown as mean ± s.e.m. of duplicate measurements. A representative donor of n = 5 donors is shown. Black columns show unactivated and white columns activated conditions in the presence of vehicle control. (**c**) Concentration-dependent inhibition by CGI1746 in primary human monocytes of soluble immune complex–triggered phosphorylation of Btk Tyr223, Btk Tyr551, PLCγ2 Tyr1217 (2 min stimulation), Erk Thr202 and Tyr204 (5 min stimulation), JNK Thr183 and Tyr185, and p38 Thr180 and Tyr182 (10 min stimulation). A representative experiment of three experiments is shown. Quantification and full blots in **Supplementary Figure 12**. (**d**) Calcium mobilization by FcγRIIa in monocytes. Monocytes were activated with anti-FcγRIIa monoclonal antibodies and then cross-linked with goat anti-mouse F(ab')$_2$ in the presence of indicated CGI1746 concentrations. Arrows indicate stimulus added.

A-loop conformation has been noted previously[20,21], this is the first case in which the binding pockets created by this fold have been exploited with a ligand to deliver exquisite selectivity. Occupation of the H3 pocket is an absolute requirement for both potency and selectivity within this chemotype, and the unusual bifurcated hydrogen bond between the amide carbonyl and Lys430 and a water molecule plays an important role in positioning the t-butylphenyl group in this pocket. The H3 pocket itself is highly sensitive to the size, shape and polarity of the amide substituent. In contrast, the aromatic ring bearing the morpholino-amide projects toward solvent (**Fig. 2a**) and accommodates a wide variety of substituents without any erosion of selectivity. Thus, the H3 pharmacophore provides a selectivity foundation for compound design strategies to optimize other parameters such as physicochemical and absorption, distribution, metabolism and elimination properties.

The binding mode of CGI1746 is distinct from that of both type I kinase inhibitors such as dasatinib and type II inhibitors such as lapatinib[30,31]. In particular, the Btk H3 pocket differs from the allosteric site occupied by type II inhibitors[30] in its relationship to the Lys430-Asp539 salt bridge. For type II binders such as lapatinib, the salt bridge facilitates access to an allosteric pocket sequestered from solvent, whereas the H3 pocket occupied by CGI1746 is located on the solvent accessible side of the Lys430-Asp539 salt bridge and thus is physically and chemically distinct from the type II allosteric site. Furthermore, although most type II compounds (but not lapatinib) bind to a DFG-out conformation of the kinase, CGI1746 binds to Btk in a DFG-in conformation with Phe540 packed toward the interior of Btk. The difference in binding mode is also reflected in off-rates. In contrast to lapatinib, which has a slower off-rate than a type I inhibitor with similar affinity[31], CGI1746 has a comparable off-rate to the type I inhibitor dasatinib with unphosphorylated Btk (**Supplementary Table 6**). Thus CGI1746 has a distinct binding mode from type II inhibitors, while exploiting the same principle of ATP-competitive hinge binding combined with an adjacent selectivity pocket to generate potency and selectivity.

CGI1746 blocked all Btk-dependent signaling events in human and murine B cells including BCR-induced Btk Tyr223 autophosphorylation and PLCγ2 Tyr1217 phosphorylation, as well as BCR-induced Ca^{2+} flux. In addition, activation of Erk, Jnk and p38 was partially inhibited, as was nuclear translocation of RelA and c-rel in primary human and mouse B cells. Taken together, these results confirm the essential role of Btk in BCR responses leading to Ca^{2+} flux and activation of the classical NFkB pathway[13,23,32,33]. Our studies also specify PLCγ2 Tyr1217 as a major substrate of Btk following BCR stimulation[23,33,34]. Furthermore, Btk inhibition blocked B cell proliferation in both IgM^+ as well as isotype-switched IgG^+ B cells, indicating that Btk inhibition has the potential to block memory B cell function during autoimmune responses.

We have identified Btk as an essential downstream mediator of immune complex–activated FcγRIII and FcγRIIA leading to Ca^{2+} flux and inflammatory cytokine production, including TNFα in murine macrophages and human monocytes, respectively. These findings have direct relevance to immune complex signaling in rheumatoid arthritis, as anti-CCP or anti-collagen autoantibodies isolated from rheumatoid arthritis patients trigger TNFα production in macrophages or monocytes through FcγRIIa[35,36]. Although Btk is also essential for FcγRIII- or FcγRIIa-induced IL-1β production in murine macrophages and human monocytes, respectively, the influence of Btk on IL-6 production in human monocytes (three- to eight-fold higher IC_{50}) compared to murine macrophages is less pronounced. Divergent regulation of TNFα and IL-6 has been reported previously, including results from TLR4-activated XLA peripheral blood mononuclear cells or Btk siRNA–treated human macrophages that show reduced TNFα production but no effect on IL-6 production[37,38]. Furthermore, selective impairment of IL-6 production suggests existence of different intracellular signaling networks in human monocytes versus murine macrophages. In this respect, we did not observe inhibition of TNFα or IL-6 production in response to TLR2 or TLR4 activation in murine macrophages (**Supplementary Fig. 8a**,**b**). Our examination of the signaling pathways downstream of Btk in human monocytes and murine macrophages, showed that although Btk enzymatic activity is crucial in both cells for immune complex–induced activation of PLCγ2 and Ca^{2+} flux, Btk contributes to Erk, Jnk and p38 activation in human monocytes (**Fig. 7c** and **Supplementary Fig. 11d**) but not significantly to Erk or Jnk phosphorylation in bone marrow-derived macrophages (BMM) (**Supplementary Fig. 6e**). A detailed assessment of the signaling pathways leading to cytokine production was beyond the scope of this manuscript; however, there are at least three potential causes for the differing production of cytokines: (i) selective contributions to transcription factor regulation, including NFAT- and NFκB-mediated gene expression, (ii) effects on post-transcriptional control of cytokines and (iii) secondary autocrine effects.

In rodent models of inflammatory arthritis, selective Btk inhibition is efficacious during both the initiation phase, when adaptive immune responses and B cells drive disease progression, and the effector phase, when inflammatory mediators including TNFα, IL-1β and IL-6 produced by myeloid cells orchestrate joint destruction. The efficacy of CGI1746 in the prophylactic CIA model is comparable to anti-CD20–induced B cell depletion or co-stimulation blockade by CTLA4-Ig and is in agreement with studies previously reported in *xid* mice[25,39,40]. Autoantigen challenge in B cell–depleted mice results in reduced antigen-specific $CD4^+$ T cell activation[41], underlining a significant contributory role for B cells in autoimmune disease initiation, which likely derives from their antigen presentation and co-stimulation functions. In this regard it has been reported that Btk regulates B cell antigen presentation function[42], levels of the co-stimulatory molecule CD86 (ref. 43) and is also important for T-independent immune responses[13]; therefore, Btk inhibition likely contributes on several levels to the efficacy in the prophylactic CIA model and the associated reduction in autoantibodies. In contrast to CIA in mice, where disease requires B cells for induction, the observed clinical benefits from rituximab therapy suggest that B cells continuously augment T cell activation in response to unremitting autoantigen challenge in rheumatoid arthritis.

We have demonstrated that Btk inhibition is efficacious in lymphocyte-independent arthritis using two passive arthritis models (CAIA, K/BxN) and during the effector phase of CIA. Specifically, the CAIA model was carried out in SCID mice to unequivocally demonstrate that Btk has an essential role in disease pathogenesis that is independent of B cells. Efficacy in the CAIA model correlated with a reduction in rheumatoid-associated inflammatory cytokines within joints. All three models have been shown to be dependent on activating FcγR, with FcγRIII and $IgG1^+$ autoantibodies playing a dominant role[8,44]. Because CGI1746 blocked production of TNFα, IL-1β and IL-6 in response to FcγRIII-mediated immune complex activation in macrophages, it is likely that the therapeutic effect of Btk inhibition is also mediated by inhibition of FcγRIII function in macrophages *in vivo*. The importance of FcγRIII expression by macrophages has been established by the adoptive transfer of $FcγRIII^+$ peritoneal macrophages, which renders $FcγRIII^{-/-}$ mice susceptible to CIA[45]. Furthermore, mice depleted of macrophages by clodronate liposome treatment are completely resistant to K/BxN serum-induced arthritis[46]. As Btk also functions in neutrophils, mast cells and osteoclasts[14,15,47–49], it is possible that Btk inhibition in these cells contributes to efficacy as well.

Genetic evidence suggests that Btk may be an attractive target for autoimmune and inflammatory diseases. However, genetic versus pharmacological inactivation can lead to different conclusions regarding the biological function of a given target[50]. Our understanding of Btk biology on the basis of the genetic

data from Btk-deficient animals is confounded by developmental defects in both B cell and myeloid cell lineages[11,13,47]. We have leveraged the high selectivity of the Btk inhibitor, CGI1746, to demonstrate that exclusive inhibition of Btk enzyme activity is sufficient to suppress BCR and FcγR signaling and function. This translates to efficacy in distinct inflammatory arthritis models that are dependent on lymphoid and/or myeloid cell function. In a complex disease state, Btk inhibition therefore has the potential to simultaneously disrupt several pathogenic pathways. These findings suggest that selective pharmacological inhibition of Btk is an attractive therapeutic strategy for rheumatoid arthritis and other autoimmune disorders. The binding mode of the Btk inhibitor chemotype disclosed herein could be broadly exploited in the design of selective inhibitors with potential application in autoimmune and inflammatory disease.

METHODS

Chemical synthesis. See the **Supplementary Methods** for synthetic procedures and characterization data.

CGI1746. CGI1746 was dissolved in DMSO for *in vitro* studies and dosed at 100 mg kg^{-1} BID SC in 20% (v/v) cremophor, 10% (v/v) ethanol and 70% (v/v) saline for *in vivo* studies.

Biochemical assays. Lanthascreen assay was performed at K_m for ATP (10 μM) with human full-length Btk (C-terminal V5-His_6 expressed in Sf9 cells) and quantified on an EnVision (Perkin Elmer).

Crystallization. Btk was expressed in insect cells, and the Btk–CGI1746, apo Btk and Btk–dasatinib structures were solved by molecular replacement to a resolution of 1.8 Å, 2.3 Å and 1.95 Å and refined to R, R_{free} values of 18.3, 21.3; 19.6, 23.0; and 22.2, 27.8% respectively.

Cell isolation. Human B cells, T cells or monocytes were purchased or isolated from peripheral blood mononuclear cells by Ficoll-Hypaque and negatively selected by magnetic cell sorting (Miltenyi Biotec). B cells from human tonsil cell suspensions were positively selected on $CD27^+$ microbeads. Murine splenic lymphocytes were isolated by negative selection. BMM were generated by culturing murine bone marrow cells with 10 ng ml^{-1} M-CSF for 7 d.

Cell stimulations. B cells or monocytes were preincubated with CGI1746 for 1 h. B cells were stimulated with 10 μg ml^{-1} anti-IgM $F(ab')_2$ or anti-IgG $F(ab')_2$ and monocytes with 40 μg ml^{-1} soluble immune complexes (1:3 ratio IgG Fc/anti-human IgG) or immobilized HSA/anti-HSA immune complexes. For western blotting, BMM were pretreated with CGI1746, cooled on ice, incubated with 5 μg ml^{-1} anti-FcγRIII or isotype control monoclonal antibodies and stimulated by cross-linking with 10 μg ml^{-1} anti-IgG $F(ab')_2$. For cytokine production, BMM were dislodged, pretreated with CGI1746 for 10 min and stimulated overnight with immobilized anti-FcγRIII monoclonal antibodies.

Cell lysis and western blotting. Cells were lysed in Cell Signaling or RIPA lysis buffer. Nuclear extracts were prepared with NE-PER (Pierce). Proteins were separated by SDS-PAGE and blots probed with commercially available antibodies and detected on an Odyssey system (LI-COR Biosciences).

Calcium flux assay. Cells were incubated with 5 μM indo-1/AM for 30 min, CGI1746 for 10 min, stimulated with anti-IgM $F(ab')_2$ (B cells), anti-FcγRIIa (clone IV.3; monocytes) or anti-FcγRIII (clone 3296; BMM) monoclonal antibodies at 0.1 μg ml^{-1} followed by anti-IgG $F(ab')_2$ (10 μg ml^{-1}). Calcium release was monitored by flow cytometry.

Proliferation assays. Lymphocytes were loaded with carboxyfluorescein succinimidyl ester (CFSE) and stimulated as outlined, and cell divisions were assessed after 3 d by fluorescence-activated cell sorting. Purified $CD27^+$ B cells were stimulated for 72 h and pulsed before harvest with 1 μCurie per well ^{3}H-thymidine. The incorporated radioactivity was then measured.

Cytokine measurements. TNFα, IL-1β, IL-6, MCP-1 and MIP-1α levels were determined by Luminex (Affymetrix, Inc.) or ELISA.

Collagen-induced arthritis. Arthritis was induced in B10RIII mice at Bolder Biopath by injecting 150 μl Complete Freund's Adjuvant (CFA) containing bovine type II collagen (2 mg ml^{-1}) (Elastin) plus mycobacterium tuberculosis H37RA on days 0 and 15. For studies at Genentech, DBA/J were immunized intradermally at the base of the tail with 100 μg bovine collagen type II (Chondrex) emulsified in 100 μl CFA on day 0; on day 21, mice were challenged with 100 μg collagen type II in 100 μl Incomplete Freund's Adjuvant (IFA). For rat CIA, female Lewis rats were injected at Bolder Biopath with 300 μl IFA containing 2 mg ml^{-1} bovine type II collagen on days 0 and 6. Measurable signs of arthritis typically develop 1–7 days after the secondary immunization. Animals were randomized and dosed with CGI1746, vehicle control or mTNFRII-Fc as indicated. Dosing starts were day 12 (prophylactic, B10RIII), day 24 (preventive, DBA/J) and after arthritis onset days 15–23 (therapeutic, B10RIII), days 7–12 (therapeutic, Lewis rat). Clinical scores or caliper measurements were recorded on days indicated. Two standard scoring systems for clinical scores were used according to the site where the studies were conducted and are outlined in **Supplementary Methods**. Serum samples were analyzed for anti-type II collagen by ELISA as indicated. Micro-CT imaging and histological examination of arthritic joints was performed as described in **Supplementary Methods**.

CAIA, K/BxN and quantification of cytokines within joints. Arthritis was induced at Genentech in CB-17 SCID mice (CAIA) by injecting 2 mg of a cocktail of arthritogenic monoclonal antibodies (Anthrogen) intravenously, followed 3 d later by intraperitoneal injection of 50 μg LPS; and in Balb/c mice (K/BxN) by injection of 100 μl pooled serum obtained from a cohort of K/BxN mice as described in **Supplementary Methods**. Clinical scoring was performed as described in **Supplementary Methods**. For the CAIA, one hindpaw from each mouse was harvested on day 11 for RNA- and protein-level analyses, respectively. For protein analyses, paws were homogenized in cell lysis buffer, cytokine concentrations determined and protein concentrations normalized to the optical density level of β-actin in each sample measured with an ELISA kit. Total cellular RNA was reverse transcribed and analyzed by one-step real-time PCR. Samples were normalized to RPL19 to obtain delta Ct values.

IC_{50} determination. IC_{50}s were determined with GraphPad Prism v5.

Statistical analysis. Statistical analysis was performed using JMP v.6.0.3 software and Dunnett's method as outlined in **Supplementary Methods**.

Accession codes. Protein Data Bank: Coordinates of all Btk structures have been deposited under the following accession codes: 3OCS (Btk–CGI1746), 3OCT (Btk–dasatinib), 3P08 (apo Btk).

All animal experiments were approved by the respective Institutional Animal Care and Use Committees of Genentech, CGI Pharmaceuticals or Bolder Biopath.

Detailed methods are available in **Supplementary Methods**.

Received 3 May 2010; accepted 20 October 2010; published online 28 November 2010

References

1. Vincent, C., Nogueira, L., Clavel, C., Sebbag, M. & Serre, G. Autoantibodies to citrullinated proteins: ACPA. *Autoimmunity* **38**, 17–24 (2005).
2. Nell, V.P. *et al.* Autoantibody profiling as early diagnostic and prognostic tool for rheumatoid arthritis. *Ann. Rheum. Dis.* **64**, 1731–1736 (2005).
3. Cook, A.D., Rowley, M.J., Mackay, I.R., Gough, A. & Emery, P. Antibodies to type II collagen in early rheumatoid arthritis. Correlation with disease progression. *Arthritis Rheum.* **39**, 1720–1727 (1996).
4. Panayi, G.S. B cell-directed therapy in rheumatoid arthritis–clinical experience. *J. Rheumatol. Suppl.* **73**, 19–24 discussion 29–30 (2005).
5. Nimmerjahn, F. & Ravetch, J.V. Fcgamma receptors as regulators of immune responses. *Nat. Rev. Immunol.* **8**, 34–47 (2008).
6. Takai, T. Roles of Fc receptors in autoimmunity. *Nat. Rev. Immunol.* **2**, 580–592 (2002).
7. Thabet, M.M. *et al.* Contribution of Fcgamma receptor IIIA gene 158V/F polymorphism and copy number variation to the risk of ACPA-positive rheumatoid arthritis. *Ann. Rheum. Dis.* **68**, 1775–1780 (2009).
8. Boross, P. & Verbeek, J.S. The complex role of Fcgamma receptors in the pathology of arthritis. *Springer Semin. Immunopathol.* **28**, 339–350 (2006).
9. Hamilton, J.A. & Tak, P.P. The dynamics of macrophage lineage populations in inflammatory and autoimmune diseases. *Arthritis Rheum.* **60**, 1210–1221 (2009).
10. Tsukada, S., Rawlings, D.J. & Witte, O.N. Role of Bruton's tyrosine kinase in immunodeficiency. *Curr. Opin. Immunol.* **6**, 623–630 (1994).
11. Satterthwaite, A.B. & Witte, O.N. The role of Bruton's tyrosine kinase in B-cell development and function: a genetic perspective. *Immunol. Rev.* **175**, 120–127 (2000).
12. Lindvall, J.M. *et al.* Bruton's tyrosine kinase: cell biology, sequence conservation, mutation spectrum, siRNA modifications, and expression profiling. *Immunol. Rev.* **203**, 200–215 (2005).
13. Khan, W.N. Regulation of B lymphocyte development and activation by Bruton's tyrosine kinase. *Immunol. Res.* **23**, 147–156 (2001).
14. Schmidt, U., Boucheron, N., Unger, B. & Ellmeier, W. The role of Tec family kinases in myeloid cells. *Int. Arch. Allergy Immunol.* **134**, 65–78 (2004).
15. Brunner, C., Muller, B. & Wirth, T. Bruton's Tyrosine Kinase is involved in innate and adaptive immunity. *Histol. Histopathol.* **20**, 945–955 (2005).

16. Currie, K.S., DeSimone, R.W., Mitchell, S.A. & Pippin, D.A. Certain heterocyclic substituted imidazo[1,2-a]pyrazin-8-yl compounds and methods of inhibition of Bruton's tyrosine kinase by such compounds. US Patent 7,393,848 (2008).
17. Brittelli, D.R. *et al.* Certain substituted amides, methods of making and methods of use thereof. World Intellectual Property Organization Patent WO/2006/099075 (2006).
18. Pan, Z. Bruton's tyrosine kinase as a drug discovery target. *Drug News Perspect.* **21**, 357–362 (2008).
19. Lin, L. *et al.* Activation loop phosphorylation modulates Bruton's tyrosine kinase (Btk) kinase domain activity. *Biochemistry* **48**, 2021–2032 (2009).
20. Schindler, T. *et al.* Crystal structure of Hck in complex with a Src family-selective tyrosine kinase inhibitor. *Mol. Cell* **3**, 639–648 (1999).
21. Marcotte, D.J. *et al.* Structures of human Bruton's tyrosine kinase in active and inactive conformations suggest a mechanism of activation for TEC family kinases. *Protein Sci.* **19**, 429–439 (2010).
22. Karaman, M.W. *et al.* A quantitative analysis of kinase inhibitor selectivity. *Nat. Biotechnol.* **26**, 127–132 (2008).
23. Watanabe, D. *et al.* Four tyrosine residues in phospholipase C-gamma 2, identified as Btk-dependent phosphorylation sites, are required for B cell antigen receptor-coupled calcium signaling. *J. Biol. Chem.* **276**, 38595–38601 (2001).
24. Yanaba, K. *et al.* B-lymphocyte contributions to human autoimmune disease. *Immunol. Rev.* **223**, 284–299 (2008).
25. Jansson, L. & Holmdahl, R. Genes on the X chromosome affect development of collagen-induced arthritis in mice. *Clin. Exp. Immunol.* **94**, 459–465 (1993).
26. Jongstra-Bilen, J. *et al.* Dual functions of Bruton's tyrosine kinase and Tec kinase during Fcgamma receptor-induced signaling and phagocytosis. *J. Immunol.* **181**, 288–298 (2008).
27. Kagari, T., Tanaka, D., Doi, H. & Shimozato, T. Essential role of Fc gamma receptors in anti-type II collagen antibody-induced arthritis. *J. Immunol.* **170**, 4318–4324 (2003).
28. Kagari, T., Doi, H. & Shimozato, T. The importance of IL-1 beta and TNF-alpha, and the noninvolvement of IL-6, in the development of monoclonal antibody-induced arthritis. *J. Immunol.* **169**, 1459–1466 (2002).
29. Katschke, K.J. Jr. *et al.* A novel inhibitor of the alternative pathway of complement reverses inflammation and bone destruction in experimental arthritis. *J. Exp. Med.* **204**, 1319–1325 (2007).
30. Liu, Y. & Gray, N.S. Rational design of inhibitors that bind to inactive kinase conformations. *Nat. Chem. Biol.* **2**, 358–364 (2006).
31. Wood, E.R. *et al.* A unique structure for epidermal growth factor receptor bound to GW572016 (Lapatinib): relationships among protein conformation, inhibitor off-rate, and receptor activity in tumor cells. *Cancer Res.* **64**, 6652–6659 (2004).
32. Marshall, A.J., Niiro, H., Yun, T.J. & Clark, E.A. Regulation of B-cell activation and differentiation by the phosphatidylinositol 3-kinase and phospholipase Cgamma pathway. *Immunol. Rev.* **176**, 30–46 (2000).
33. Humphries, L.A. *et al.* Tec kinases mediate sustained calcium influx via site-specific tyrosine phosphorylation of the phospholipase Cgamma Src homology 2-Src homology 3 linker. *J. Biol. Chem.* **279**, 37651–37661 (2004).
34. Kim, Y.J., Sekiya, F., Poulin, B., Bae, Y.S. & Rhee, S.G. Mechanism of B-cell receptor-induced phosphorylation and activation of phospholipase C-gamma2. *Mol. Cell. Biol.* **24**, 9986–9999 (2004).
35. Mullazehi, M., Mathsson, L., Lampa, J. & Ronnelid, J. Surface-bound anti-type II collagen-containing immune complexes induce production of tumor necrosis factor alpha, interleukin-1beta, and interleukin-8 from peripheral blood monocytes via Fc gamma receptor IIA: a potential pathophysiologic mechanism for humoral anti-type II collagen immunity in arthritis. *Arthritis Rheum.* **54**, 1759–1771 (2006).
36. Clavel, C. *et al.* Induction of macrophage secretion of tumor necrosis factor alpha through Fcgamma receptor IIa engagement by rheumatoid arthritis-specific autoantibodies to citrullinated proteins complexed with fibrinogen. *Arthritis Rheum.* **58**, 678–688 (2008).
37. Horwood, N.J. *et al.* Bruton's tyrosine kinase is required for TLR2 and TLR4-induced TNF, but not IL-6, production. *J. Immunol.* **176**, 3635–3641 (2006).
38. Palmer, C.D. *et al.* Bmx tyrosine kinase regulates TLR4-induced IL-6 production in human macrophages independently of p38 MAPK and NFkapp. *Blood* **111**, 1781–1788 (2008).
39. Yanaba, K. *et al.* B cell depletion delays collagen-induced arthritis in mice: arthritis induction requires synergy between humoral and cell-mediated immunity. *J. Immunol.* **179**, 1369–1380 (2007).
40. Knoerzer, D.B., Karr, R.W., Schwartz, B.D. & Mengle-Gaw, L.J. Collagen-induced arthritis in the BB rat. Prevention of disease by treatment with CTLA-4-Ig. *J. Clin. Invest.* **96**, 987–993 (1995).
41. Bouaziz, J.D. *et al.* Therapeutic B cell depletion impairs adaptive and autoreactive $CD4^+$ T cell activation in mice. *Proc. Natl. Acad. Sci. USA* **104**, 20878–20883 (2007).
42. Sharma, S., Orlowski, G. & Song, W. Btk regulates B cell receptor-mediated antigen processing and presentation by controlling actin cytoskeleton dynamics in B cells. *J. Immunol.* **182**, 329–339 (2009).
43. Goldstein, M.D., Debenedette, M.A., Hollenbaugh, D. & Watts, T.H. Induction of costimulatory molecules B7–1 and B7–2 in murine B cells. the CBA/N mouse reveals a role for Bruton's tyrosine kinase in CD40-mediated B7 induction. *Mol. Immunol.* **33**, 541–552 (1996).
44. Monach, P.A., Benoist, C. & Mathis, D. The role of antibodies in mouse models of rheumatoid arthritis, and relevance to human disease. *Adv. Immunol.* **82**, 217–248 (2004).
45. Andrén, M., Xiang, Z., Nilsson, G. & Kleinau, S. FcgammaRIII-expressing macrophages are essential for development of collagen-induced arthritis. *Scand. J. Immunol.* **63**, 282–289 (2006).
46. Solomon, S., Rajasekaran, N., Jeisy-Walder, E., Snapper, S.B. & Illges, H. A crucial role for macrophages in the pathology of K/B x N serum-induced arthritis. *Eur. J. Immunol.* **35**, 3064–3073 (2005).
47. Mangla, A. *et al.* Pleiotropic consequences of Bruton tyrosine kinase deficiency in myeloid lineages lead to poor inflammatory responses. *Blood* **104**, 1191–1197 (2004).
48. Lee, S.H., Kim, T., Jeong, D., Kim, N. & Choi, Y. The tec family tyrosine kinase Btk Regulates RANKL-induced osteoclast maturation. *J. Biol. Chem.* **283**, 11526–11534 (2008).
49. Shinohara, M. *et al.* Tyrosine kinases Btk and Tec regulate osteoclast differentiation by linking RANK and ITAM signals. *Cell* **132**, 794–806 (2008).
50. Knight, Z.A. & Shokat, K.M. Chemical genetics: where genetics and pharmacology meet. *Cell* **128**, 425–430 (2007).

Acknowledgments

We thank H. Nguyen (Genentech) for data analyses and graphing; E. Suto, M. Zhou, Z. Huang and Translational Immunology at Genentech for animal studies; X. Qian (CGI) for initiation of first efficacy studies; T. Stephan (CGI), H. La, L. Liu and H. Wong (Genentech) for pharmacokinetic analyses; the Genentech Baculovirus Expression Group for recombinant Btk proteins; R. Zabinski (Emerald BioStructures) for purification of Btk for the Btk–CGI1746 and Btk–dasatinib crystal structures; L. Lubach, V. Nguyen and M. Xie (Genentech) for formulation support; L. Gilmour, R. Neupane and J. Cupp (Genentech) for fluorescence-activated cell sorting support; F. Shen (Genentech) for help with primary cell cultures; A. Nguyen (Genentech) for antibody titer analyses; H. Chiu (Genentech) for help with Luminex assays; K. Dodge, N. Chiang, K. McCutcheon, K. Schroeder, J. Hongo, M. Hazen and Antibody Engineering at Genentech for antibody support; P. Caplazi (Genentech) for histology support; M. Navia for advice on cocrystallization conditions; M. Velleca and D. Armistead for valuable advice; and F. Martin and H. Singh for manuscript critique.

Author contributions

J.A.D.P. supervised the biology, analyzed data and contributed to the manuscript; T.H. performed *in vitro* assays, western blot analyses, and end point analyses from *in vivo* studies and contributed to the methods section; J.D., J.E.K. and S.A.M. designed and synthesized compounds; J.B. supervised CGI arthritis studies and performed analyses; P.G., J.Z. and W.P.L. performed GNE arthritis studies; M.B. supervised GNE *in vivo* studies; V.H. contributed to testing of antibodies and performed proliferation assays; R.J. performed proliferation assays; H.R. performed western blot analyses; L.D. and R.F. performed histology; R.A.D.C. and K.H.B. performed microcomputed tomographic imaging and analysis; S.Y. and L.E.D. performed Luminex assays and analyses; P.M.M. performed biochemical assays; W.B.Y. coordinated the collaborative effort; J.A.W. contributed to the design of the cloning and expression strategies for Btk constructs; D.R.D. and B.L.S. expressed Btk-KD, crystallized Btk with CGI1746 and dasatinib and solved the structures; A.M.G. supervised and performed analysis, and B.J.B. conducted surface plasmon resonance studies; C.Y. purified and crystallized apo Btk; S.L.G. supervised crystallography studies at CGI; S.G.H. solved apo Btk structure and contributed to the manuscript; K.S.C. designed and synthesized compounds, led the drug discovery program and contributed to the manuscript; K.R. led and supervised biology research, designed experiments and wrote the manuscript.

Competing financial interests

The authors declare competing financial interests: details accompany the full-text HTML version of the paper at http://www.nature.com/naturechemicalbiology/.

Additional information

Supplementary information and chemical compound information is available online at http://www.nature.com/naturechemicalbiology/. Reprints and permissions information is available online at http://npg.nature.com/reprintsandpermissions/. Correspondence and requests for materials should be addressed to K.R. or K.S.C.